The Journey of Lithium

Laura Magrini[1]
Rodolfo Smiljanic[2]
Nadège Lagarde[3, 4]
Elena Franciosini[1]
Luca Pasquini[5]
Donatella Romano[6]
Sofia Randich[1]
Gerry Gilmore[7]

[1] INAF – Astronomical Observatory of Arcetri, Florence, Italy
[2] Nicolaus Copernicus Astronomical Center, Polish Academy of Sciences, Warsaw, Poland
[3] UTINAM Institute, CNRS UMR 6213, University of Bourgogne Franche-Comté and Besançon Observatory, France
[4] LAB CNRS, University of Bordeaux, France
[5] ESO
[6] INAF – Astrophysics and Space Science Observatory of Bologna, Italy
[7] Institute of Astronomy, University of Cambridge, UK

Figure 1. The evolution of the lithium abundance A(Li) across the surface gravity–effective temperature (Kiel) diagram from the sixth Gaia–ESO internal data release.

After more than ten years and six data releases, the Gaia–ESO spectroscopic survey has come to an end. Gaia–ESO provides an extremely rich database of stellar parameters, radial velocities, and chemical abundances of more than 100 000 stars, amongst which the abundance of lithium can be considered one of the main products. Lithium is perhaps the most enigmatic of the elements, with several open issues regarding its nucleosynthesis and its evolution in stars and in the Galaxy. Gaia–ESO observations are allowing such issues to be addressed, by providing lithium abundances in stars from the pre-main sequence, through the main sequence, up to the red giant branch and the helium-burning red clump phase, over a wide range of masses. In the present work, we discuss the journey of lithium on the surface of evolved stars, using Gaia–ESO data for both field and cluster stars. We focus on the impact of extra mixing and possible lithium enrichment during the helium-burning phase. We briefly comment on the implications that these results may have for models of the chemical evolution of lithium in the Galaxy.
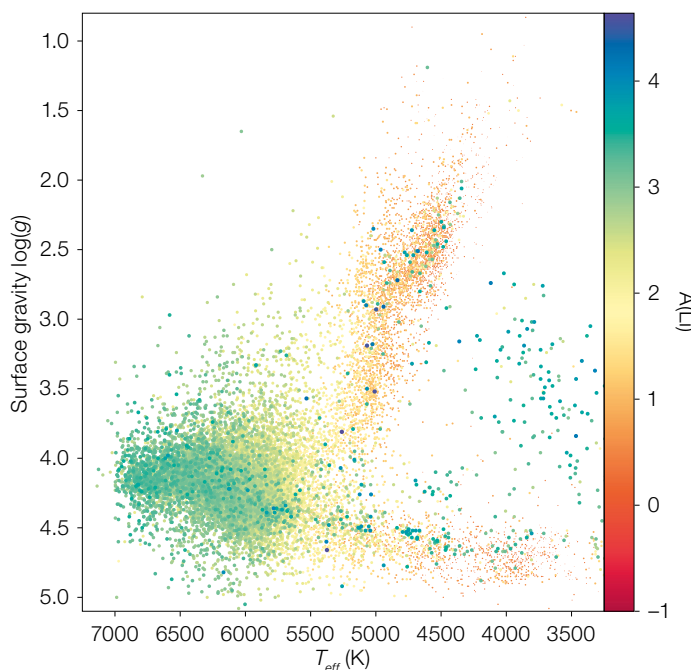
Introduction

Since the latest internal data release of the Gaia–ESO spectroscopic survey[1] in December 2020, many topics related to lithium (Li) abundances have been addressed by the Gaia–ESO collaboration. Recent publications include the serendipitous discovery of a rare Li-rich giant in the globular cluster NGC 1206 (Sanna et al., 2020), the study of the Galactic evolution of Li (Randich et al., 2020; Romano et al., 2021), the use of Li as an age tracer (Gutierrez Albarran et al., 2020; Binks et al., 2021), the exploitation of Li to put constraints on pre-main sequence evolutionary models and the effect of magnetic activity (Franciosini et al., submitted to *Astronomy and Astrophysics*), and the study of mixing processes in giant stars using Li as a tracer (Magrini et al., 2021a,b). We refer to Randich & Magrini (2021) for a description of the potential of the Gaia–ESO Survey data for Li studies. Figure 1 plots surface gravity against effective temperature (sometimes called a Kiel diagram) for all stars in the final data release of the Gaia–ESO Survey for which Li was measured. The figure highlights the data coverage in terms of evolutionary stages.

Of all the elements in the periodic table, Li, in the form of its main isotope ^{7}Li, has the most complex origin and evolution (see Romano et al., 2021). Li is one of the few elements, along with H and He, produced in the first instants of the Universe, by primordial nucleosynthesis after the Big Bang. However, the Li abundance we measure today is only in part the primordial one, because many destructive and constructive processes have occurred since (see, for example, Matteucci, D'Antona & Timmes, 1995; Romano et al., 2021; Randich & Magrini, 2021).

The production channels of Li include: stellar nucleosynthesis through the intermediate production of ^{7}Be, which is carried by convection to cooler stellar layers where it decays to ^{7}Li — the so-called Cameron-Fowler (CF) mechanism (Cameron & Fowler, 1971); thermonuclear runaways during classical nova explosions (Arai et al., 2021); Li production triggered by the flux of neutrinos emerging from the collapsing cores of exploding massive stars (Sieverding et al., 2018); and spallation of interstellar medium atoms by high-energy Galactic cosmic rays (Meneguzzi, Audouze & Reeves, 1971). However, as stated by Romano et al. (2021), *"it is a little disconcerting that none of the proposed ^{7}Li production channels have been firmly assessed yet"*. To shed light on the production of Li, all these mechanisms are considered by

Romano et al. (2021), who compare Gaia–ESO data with a model of chemical evolution. This comparison shows that most of the production of Li likely comes from nova outbursts, with the usual caution related to the non-uniqueness of the solution.

On the other hand, Li is easily destroyed in stellar interiors by proton capture at relatively low temperatures (~ 2.5 million K). Several transport mechanisms, such as convection, atomic diffusion, overshooting, rotation-induced mixing, mixing by internal gravity waves or magnetohydrodynamic instabilities, might circulate material into these hotter layers, where Li is burned, and then up to the surface, resulting in the dilution of photospheric Li. The destruction of Li is particularly important after the main sequence (MS), when convection dominates the stellar envelopes and dilutes the Li abundance by a factor of 30 to 60 from the initial abundance (the so-called first dredge-up[a]; see Iben, 1967). Additional physical mechanisms, not included in standard evolutionary models, can cause further dilution of Li down to very low abundance values in the subsequent evolution of a star. These likely depend on the initial metallicity, mass and rotation of the star as well as other stellar properties, which still remain poorly understood if not uncomfortably unknown (see, for example, Anthony-Twarog et al., 2018; Charbonnel et al., 2021).

In this article, we will focus on the evolution of Li after the MS, where mostly destructive processes take place, but where some unexpected production can also happen. The results are described in detail in Magrini et al. (2021a,b).

The post-MS evolution of Li: catching the effect of extra mixing

In our investigation of the evolution of Li after the MS, we have used the homogeneously determined Li abundances for the combined Gaia–ESO sample of open cluster and field stars. Its large database of open clusters is indeed an important difference between Gaia–ESO and other surveys. For stars that are cluster members, metallicity, age and mass can be estimated more accurately than for field

stars. This allows a more thorough comparison between the observed Li abundances and the predictions of theoretical models. The Gaia–ESO data probe Li abundances in stars with a wide range of stellar masses and metallicities. In open clusters, the giant stars range from 1.1 to 4.5 $M_\odot$. With the complement of field stars, the mass range reaches even lower values.

We have tested two sets of models from Lagarde et al. (2012): the classical ones, which include convection as the main mixing mechanism, and models that include, in addition to convection, the effects of rotation during the MS and of mixing driven by thermohaline instability[b]. The comparison with the models confirms that convection alone cannot explain the observations, and that there is a strong contribution from rotation-induced mixing in the more massive stars in our sample. For the lower-mass giant stars in clusters and in the field, the comparison provides support to the hypothesis that a mixing process in the advanced phases of stellar evolution is required. This process might be thermohaline mixing.

These results are shown in Figure 2, in which the Li abundance A(Li) in open star clusters, divided into age bins, is shown as a function of effective temperature. Convection alone cannot explain the behaviour of Li after the first dredge-up and the observed further decrease in A(Li) can only be understood with the addition of some extra mixing processes. In Figure 2 we highlight a few special stars in which A(Li) is anomalously high, the so-called Li-rich giants. They are distributed around three main locations in the Hertzprung-Russel (HR) diagram: the red giant branch (RGB) luminosity bump[c], the core-He-burning stages, and the early asymptotic giant branch. They are only a few percent of the total sample, but explaining their origin is quite challenging.

Are Li-rich giants the tip of the iceberg? Is there room for a general Li production after the RGB phase?

The existence of Li-rich giants has been known for many years (see, for example,

Brown et al., 1989; Charbonnel & Balachandran, 2000; Monaco et al., 2011; Kumar, Reddy & Lambert, 2011). However, their nature remains a mystery that has not yet been fully resolved. Usually, Li-rich giants are defined as those with A(Li) > 1.50, where this limit is the expected Li abundance after the first dredge-up. Many studies have shown that they amount to 1–2% of all red giant stars (see, for example, Casey et al., 2016; Smiljanic et al., 2018; Deepak & Reddy, 2019; Martell et al., 2020; Charbonnel et al., 2020). Recent results, based on a combination of spectroscopic and asteroseismic observations, have indicated the predominance of Li-rich giants in the core-helium-burning red clump (RC) phase (Silva Aguirre et al., 2014; Casey et al., 2019; Kumar & Reddy, 2020; Deepak & Lambert, 2021; Yan et al., 2021; Singh, Reddy & Kumar, 2019; Singh et al., 2021). Kumar et al. (2020) performed a large-scale investigation of the Li content in low-mass field stars in the RC phase. They suggest that the classical Li-rich RC giants (those with A(Li) > 1.50) are only the tip of the iceberg of a more general Li production in that phase. In their view, Li production in low-mass RC stars is actually ubiquitous. In our work, we explore this possibility from the point of view of open clusters.

Thanks to the high quality of the Gaia–ESO data, we can clearly separate RC stars from RGB stars in the HR diagram of open clusters. In Figure 3, we show the evolution of A(Li) after the MS. Following the prediction of the models (classical and with rotation and thermohaline mixing) from left to right in Figure 3 we begin with stars at the end of the MS, where A(Li) is between 2.5 and 3.4. Afterwards, the first dredge-up dilutes A(Li) at 1.3–1.5, almost independently of the stellar mass in classical models. In models with rotation and thermohaline mixing, the depletion of Li does not stop at the first dredge-up but continues: there is a further dilution at the RGB bump when the thermohaline instability is activated. After that, stars evolve towards the RGB tip and then drop in luminosity, reaching the RC. Further evolution during the RC can deplete Li down to –1 dex before the stellar luminosity increases again. The observations of stars in open clusters show that the typical A(Li) values of the
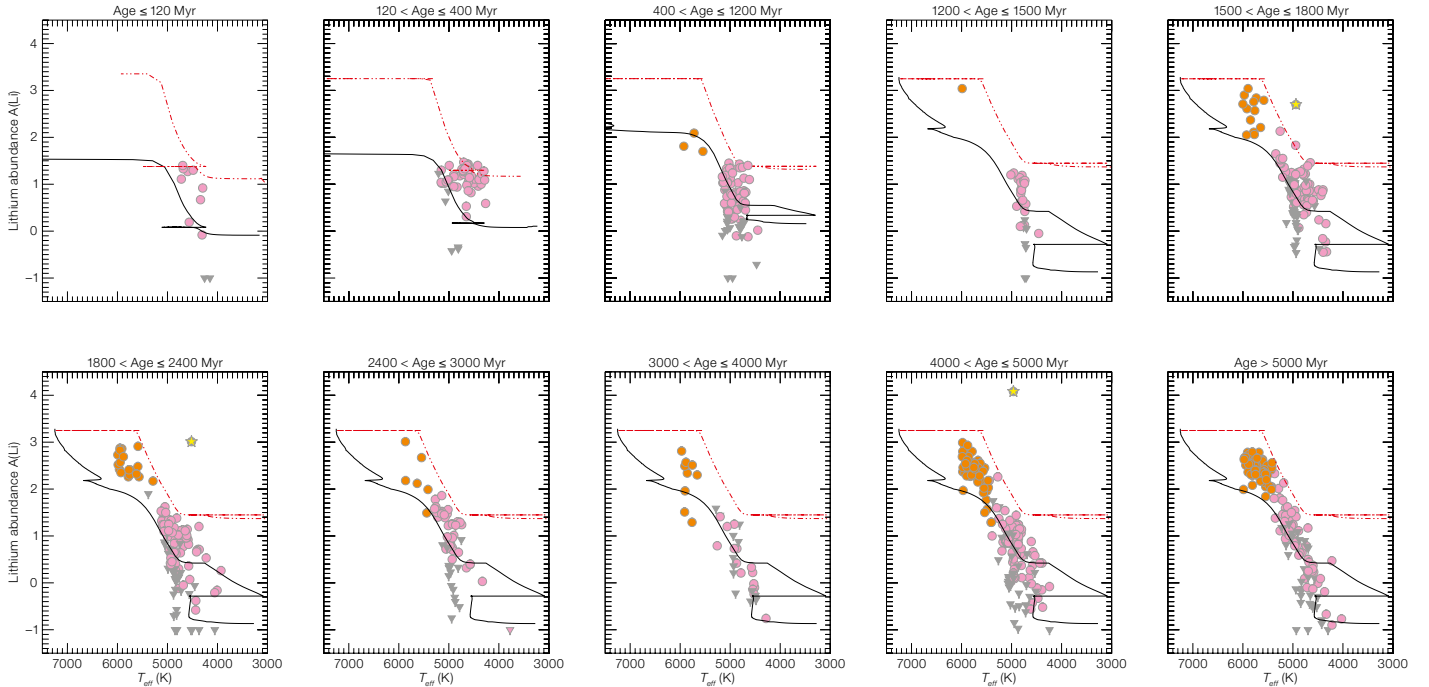
Figure 2. Lithium abundance A(Li) as a function of the effective temperature in open clusters in different age bins. The curves are the model predictions from Lagarde et al. (2012) for the closest stellar masses, with standard mixing (dashed lines) and including rotation-induced mixing (continuous lines), all for solar metallicity. The Li-rich giant stars are indicated with yellow stars.

Figure 3. Luminosity versus A(Li) of member stars of open clusters with $1\,M_\odot < M < 1.8\,M_\odot$ and $-0.2 < [Fe/H] < 0.2$. Grey circles show the whole sample of member stars and coloured circles the stars at the RC. Triangles show the upper limits on A(Li). The continuous red and green curves are the models with rotation and thermohaline mixing at solar metallicity for $1.5\,M_\odot$ and $2\,M_\odot$, respectively, while the dotted red and green curves are the standard models for the same masses from Lagarde et al. (2012). The vertical black line indicates the limit for Li-rich giants with A(Li) > 1.5, while the vertical blue line at A(Li) > 0.9 shows the RC-RGB limit of Kumar et al. (2020). The locations of the RC in the models of Lagarde et al. (2012) that include rotation and thermohaline mixing are shown with green and red arrows.
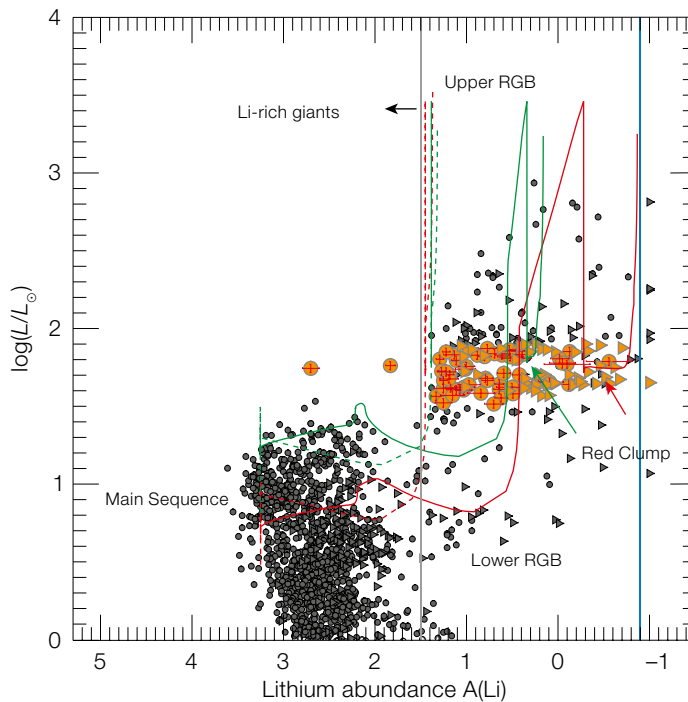
RC stars are higher than expected from the models, while the same models fairly well reproduce A(Li) in the previous RGB phases.

What happens after the RGB, in the He-burning phase?

The data from open clusters in Figure 3 suggest that a further Li enrichment occurs just before or during the RC phase in a number of RC stars. The important thing is to evaluate the frequency at

which this enrichment happens. In Figure 4 we show member stars in a representative cluster, Trumpler 5, separating them into the three evolutionary phases (RGB before and after the bump, and RC). The distribution of Li abundances in the RC stars shows values that are either similar to or even higher than those of
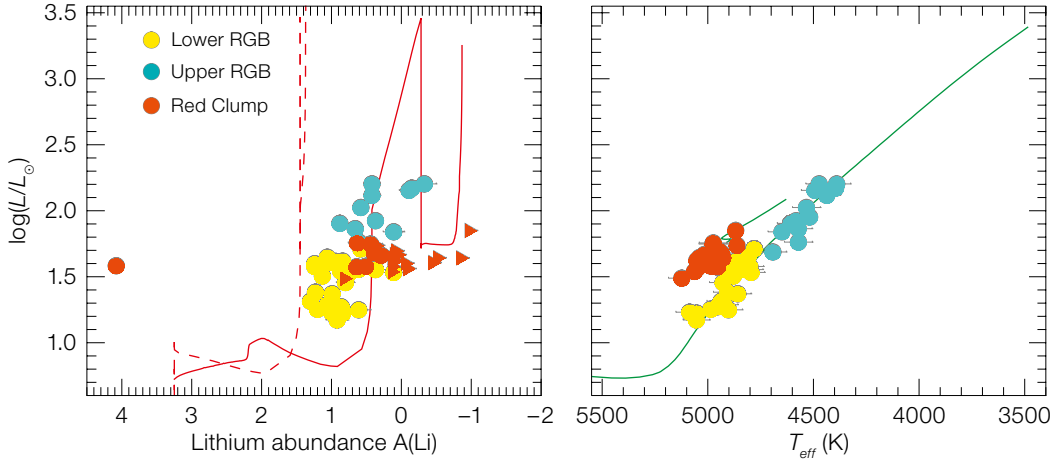
Figure 4. A(Li) and stellar parameters of member stars in the old cluster Trumpler 5. Left panels: Luminosity versus A(Li); yellow circles are lower RGB stars — prior to the RGB bump, cyan circles are upper RGB stars — after the bump, and red circles are RC stars. The continuous red curves are the models with rotation-induced mixing at solar metallicity for 1.5 $M_\odot$. The dotted red curves are the classical models with only convection from Lagarde et al. (2012). Right panels: HR diagrams with the Parsec isochrone (Bressan et al., 2012) at the age and metallicity of Trumpler 5.

the upper RGB stars. In practice, in Figure 4 we would expect RC stars to be located in the region where A(Li) reaches a plateau, with values between 0 and –1.

Considering only stars for which we provide measurements of A(Li), we find that from 35 to 50% of RC stars have A(Li) higher than stars in the previous phase, i.e., at the end of the RGB phase. Since the presence of several upper limits might hide much lower A(Li), we conclude that Li enrichment happens in a large percentage of RC stars, but that it might not be ubiquitous. The comparison with models that include additional mixing processes after the RGB phase, for instance He-flash mixing (Schwab, 2020) and neutrino momentum mixing (Mori et al., 2021), is very promising. Such models have the capacity to qualitatively explain the behaviour of the RC stars. Whilst they differ in terms of the description of the processes and their timescales, they do agree on the requirement for a mixing process during the He flash that is needed to activate the production of Li.

With the new data from Gaia–ESO, the journey of Li on the surface of evolved stars is seen to be complex. Even in evolutionary phases in which we might have expected only destructive processes, we find that Li can still be recreated. Since low-mass stars are the dominant population in the Galaxy that rules Li production at late times, this kind of production could have remarkable effects on our understanding of the whole evolutionary history of Li. In particular, we need to ascertain if Li production on the RC could

effectively compete with Li synthesis in thermonuclear nova outbursts, and this would push the quest for increasingly refined stellar and Galactic chemical evolution models.

References

Anthony-Twarog, B. J. et al. 2018, AJ, 155, 138
Arai, A. et al. 2021, ApJ, 916, 44
Binks, A. S. et al. 2021, MNRAS, 505, 1280
Bressan, A. et al. 2012, MNRAS, 427, 127
Brown, J. A. et al. 1989, ApJS, 71, 293
Cameron, A. G. W. & Fowler, W. A. 1971, ApJ, 164, 111
Casey, A. R. et al. 2016, MNRAS, 461, 3336
Casey, A. R. et al. 2019, ApJ, 880, 125
Charbonnel, C. & Balachandran, S. C. 2000, A&A, 359, 563
Charbonnel, C. et al. 2020, A&A, 633, A34
Charbonnel, C. et al. 2021, A&A, 649, L10
Deepak & Reddy, B. E. 2019, MNRAS, 484, 2000
Deepak & Lambert, D. L. 2021, MNRAS, 507, 205
Gutierrez Albarran, M. L. et al. 2020, A&A, 643, A71
Kumar, Y. B., Reddy, B. E. & Lambert, D. L. 2011, ApJL, 730, L12
Kumar, Y. B. & Reddy, B. E. 2020, Journal of Astrophysics and Astronomy, 41, 49
Kumar, Y. B. et al. 2020, Nature Astronomy, 4, 1059
Iben, I. 1967, ApJ, 147, 624

Lagarde, N. et al. 2012, A&A, 543, A108
Magrini, L. et al. 2021a, A&A, 651, A84
Magrini, L. et al. 2021b, arXiv:2108.11677
Martell, S. et al. 2020, arXiv:2006.02106
Matteucci, F., D'Antona, F. & Timmes, F. X. 1995, A&A, 303, 460
Meneguzzi, M., Audouze, J. & Reeves, H. 1971, A&A, 15, 337
Monaco, L. et al. 2011, A&A, 529, A90
Mori, K. et al. 2021, MNRAS, 503, 2746
Randich, S. & Magrini, L. 2021, Frontiers in Astronomy and Space Sciences, 8, 6
Randich, S. et al. 2020, A&A, 640, L1
Romano, D. et al. 2021, A&A, 653, A72
Sanna, N. et al. 2020, A&A, 639, L2
Schwab, J. 2020, ApJL, 901, L18
Sieverding, A. 2018, ApJ, 865, 143
Silva Aguirre, V. et al. 2014, ApJL, 784, L16
Singh, R., Reddy, B. E. & Kumar, Y. B. 2019, MNRAS, 482, 3822
Singh, R. et al. 2021, ApJL, 913, L4
Smiljanic, R. et al. 2018, A&A, 617, A4
Yan, H.-L. et al. 2021, Nature Astronomy, 5, 86

Links

[1] The Gaia–ESO spectroscopic survey:
https://www.gaia-eso.eu/

Notes

[a] The first dredge-up is the first episode of mixing occurring when a star enters the RGB, and corresponding in Figure 2 to the point in the classical models at which we have no further decrease of A(Li).
[b] Thermohaline instability arises when an unstable gradient in composition is stabilised by a gradient in temperature — it also happens on Earth, in oceanic regions where evaporation produces a warm layer of saltier water above a layer of less salty, cooler water. The two layers can exchange heat though "salt fingers", which allow the mixing.
[c] The RGB bump is the evolutionary phase in which the shell reaches the discontinuity left by the envelope causing a momentary drop in the stellar luminosity.